

A systematic evaluation of quenching and extraction procedures for quantitative metabolome profiling of Hela carcinoma cell under 2D and 3D cell culture conditions

Tong Wang¹, Xueting Wang¹, Yingping Zhuang¹, and Guan Wang¹

¹East China University of Science and Technology

August 30, 2022

Abstract

Metabolic reprogramming has been coined as a hallmark of cancer, accompanied by which the alterations in metabolite levels have profound effects on gene expression, cellular differentiation and the tumor environment. Yet a systematic evaluation of quenching and extraction procedures for quantitative metabolome profiling of tumor cells is currently lacking. To achieve this, this study is aimed at establishing an unbiased and leakage-free metabolome preparation protocol for Hela carcinoma cell. We evaluated 12 combinations of quenching and extraction methods from three quenchers (liquid nitrogen, -40°C 50% methanol, 0.5°C normal saline) and four extractants (80% methanol, methanol: chloroform: water (1:1:1, v/v/v), 50% acetonitrile, 75°C 70% ethanol) for global metabolite profiling of adherent Hela carcinoma cells. Based on the isotope dilution mass spectrometry (IDMS) method, gas/liquid chromatography in tandem with mass spectrometry was used to quantitatively determine 43 metabolites including sugar phosphates, organic acids, amino acids, adenosine nucleotides and coenzymes involved in central carbon metabolism. Among 12 combinations, cells that washed twice with phosphate buffered saline (PBS), quenched with liquid nitrogen, and then extracted with 50% acetonitrile was found to be the most optimal method to acquire intracellular metabolites with minimal loss during sample preparation. Furthermore, a case study was carried out to evaluate the effect of doxorubicin (DOX) on both adherent cells and 3D tumor spheroids using quantitative metabolite profiling. Based on this, quantitative time-resolved metabolite data can serve to the generation of hypotheses on metabolic reprogramming to reveal its important role in tumor development and treatment.

A systematic evaluation of quenching and extraction procedures for quantitative metabolome profiling of Hela carcinoma cell under 2D and 3D cell culture conditions

Tong Wang¹, Xueting Wang¹, Yingping Zhuang^{1,2}, Guan Wang^{1,2*}

1. State Key Laboratory of Bioreactor Engineering, East China University of Science and Technology (ECUST), Shanghai, People's Republic of China.

2. Qingdao Innovation Institute of East China University of Science and Technology, Shanghai,

People's Republic of China.

*Correspondence: guanwang@ecust.edu.cn

Abstract

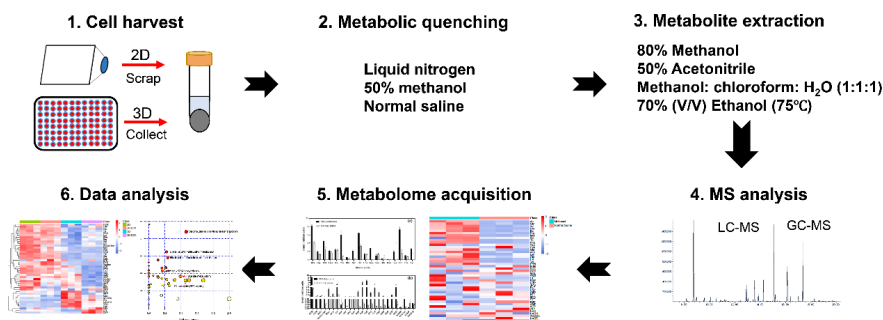
Metabolic reprogramming has been coined as a hallmark of cancer, accompanied by which the alterations in metabolite levels have profound effects on gene expression, cellular differentiation and the tumor environment. Yet a systematic evaluation of quenching and extraction procedures for quantitative metabolome profiling of tumor cells is currently lacking. To achieve this, this study is aimed at establishing an unbiased

and leakage-free metabolome preparation protocol for HeLa carcinoma cell. We evaluated 12 combinations of quenching and extraction methods from three quenchers (liquid nitrogen, -40°C 50% methanol, 0.5°C normal saline) and four extractants (80% methanol, methanol: chloroform: water (1:1:1, v/v/v), 50% acetonitrile, 75°C 70% ethanol) for global metabolite profiling of adherent HeLa carcinoma cells. Based on the isotope dilution mass spectrometry (IDMS) method, gas/liquid chromatography in tandem with mass spectrometry was used to quantitatively determine 43 metabolites including sugar phosphates, organic acids, amino acids, adenosine nucleotides and coenzymes involved in central carbon metabolism. According to the number, amount, and reproducibility of extracted metabolites, we found that 50% acetonitrile was an excellent extractant for HeLa cells while 1:1:1 methanol: chloroform: water behaved the worst extraction efficiency. The results showed that the total amount of the intracellular metabolites in cell extracts obtained using different sample preparation procedures with the IDMS method ranged from 21.51 to 295.33 nmol/million cells. Consistent with previous study, metabolite leakage was found to be maximal with cold methanol as the quencher. Among 12 combinations, cells that washed twice with phosphate buffered saline (PBS), quenched with liquid nitrogen, and then extracted with 50% acetonitrile was found to be the most optimal method to acquire intracellular metabolites with minimal loss during sample preparation. In addition, the same conclusion was drawn as these 12 combinations were applied to obtain quantitative metabolome data from three-dimensional (3D) tumor spheroids. Furthermore, a case study was carried out to evaluate the effect of doxorubicin (DOX) on both adherent cells and 3D tumor spheroids using quantitative metabolite profiling. Extracellular metabolite concentrations showed that 3D cells performed an enhanced glucose consumption and lactate excretion rate than two-dimensional (2D) cells before and after the addition of DOX. While, the addition of DOX did not interfere with extracellular glutamine concentration in both 2D and 3D cells. Pathway enrichment analysis using targeted metabolomics data showed that DOX exposure would significantly affect amino acid metabolism-related pathways, which might be related to the mitigation of redox stress. Strikingly, our data suggested that compared to 2D cells the increased intracellular glutamine level in 3D cells benefited replenishing the tricarboxylic acid (TCA) cycle when the glycolysis was limited after dosing with DOX. Taken together, this study provides a well-established quenching and extraction protocol for quantitative metabolome profiling of HeLa carcinoma cell under 2D and 3D cell culture conditions. Based on this, quantitative time-resolved metabolite data can serve to the generation of hypotheses on metabolic reprogramming to reveal its important role in tumor development and treatment.

Keywords : HeLa; metabolomics; sample preparation; 3D tumor spheroids; quenching; extraction; isotope dilution mass spectrometry

Graphical abstract

Optimized harvesting, quenching and extraction protocols for both 2D and 3D HeLa carcinoma cell metabolomics analysis.



1. Introduction

Cancer is the top two cause of death among people under the age of 70 in most countries, which has long been a serious threat to human life and health [1]. Cancer is caused by spontaneous or environmental factors

induced genetic mutations which involves abnormal cell growth with the potential to invade or spread to other parts of the body [2]. As the direct and indirect consequences of carcinogenic mutations, tumorigenesis largely depends on the reprogramming of cell metabolism with metabolic changes into six hallmarks such as dysregulated nutrient uptake kinetics, enhanced opportunistic modes of nutrient acquisition, increased use of central intermediates for biosynthesis and nicotinamide adenine dinucleotide phosphate (NADPH) production, increased demand for nitrogen, altered metabolite-driven gene regulation, and metabolic interactions with the microenvironment [3]. For example, Cairns et al found that the glucose uptake rate of tumor cells could reach about 10 times that of normal cells [4], and Patra et al. found that the expression of hexokinase 2 (HK2) was significantly up-regulated and HK2 ablation inhibited the neoplastic phenotype of human lung and breast cancer cells in vitro and in vivo [5]. Spinelli et al. found that breast cancer cells can recycle waste by-product "ammonia" as nitrogen source to promote tumor growth [6]. As a result, these specific hallmarks exhibited by an individual tumor can confer a druggable metabolic vulnerability sufficient to open a therapeutic window. For example, the expression of PUMILIO 1/2 (PUM1/2) was increased in colorectal cancer (CRC). Gong et al. found that knockdown of Pum1 and/or Pum2 in human CRC cells resulted in a significant reduction in tumorigenicity and intravenous injection of nanoparticle-encapsulated anti-Pum1 and Pum2 siRNA reduced the growth of CRC cells. These findings revealed the potential of PUM proteins as therapeutic targets for CRC [7]. Non-small-cell lung cancer (NSCLC) patients with activating epidermal growth factor receptor (EGFR) mutations developed resistance to tyrosine kinase inhibitor (TKI). Wang et al. found that EGFR C797S mutation was closely related to AXL through transcriptome and proteome analysis, and inhibition of AXL could effectively slow down the growth of NSCLC cells harboring EGFR C797S. This finding suggested that AXL inhibition might be a potential adjuvant therapy for NSCLC harboring the EGFR C797S mutation [8].

Metabolome defines a set of metabolites in a biological sample, which provides snapshots of tumor cells in response to genetic and/or therapeutic perturbations. Metabolic footprinting has been used to identify tumor biomarkers for cancer diagnosis and prognosis, and such biomarkers can be assayed in non-invasively collected biofluids like blood or serum [9-11]. Recently, the combination of cancer models with metabolomic analysis has been shown to be a powerful approach to generate new hypotheses about predicting drug susceptibility, resistance and mode of action [12]. For example, JAIN et al. found that interfering with glycine metabolism slowed the growth of rapidly proliferating cancer cells and suggested that the increased dependence of rapidly growing cancer cells on glycine might provide a potential target for therapeutic intervention [13]. Newman et al. found that cancer cells could utilize serine as a major source of carbon units and it allowed cancer cells to maintain high proliferation rates [14]. Tao et al. observed 270 dysregulated lipids in serum exosomes between pancreatic cancer (PC) patients and healthy controls through non-targeted lipidomic analysis, which might become diagnostic biomarkers [15]. Through metabolomic analysis, Bermudez et al. assessed proliferation of a collection of cancer cells following inhibition of the mitochondrial electron transport chain (ETC) and found that cell lines least sensitive to ETC inhibition maintained intracellular aspartate levels by importing it. This suggested that aspartate was the limiting metabolite for tumor growth and may be a target for cancer therapy [16].

In order to exploit pivotal intracellular mechanisms associated with tumor growth and drug resistance requires an insightful investigation of intracellular metabolites. To achieve this, sample preparation and analytical protocols should be developed and evaluated in terms of reproducibility and number of metabolite features obtained [17]. Nevertheless, acquiring metabolome changes is experimentally demanding, such that dynamic data in the development, progression and therapeutic treatment of cancer are extremely scarce. Meanwhile, achieving the absolute quantification of global metabolite is further hampered by sample pretreatment with loss and biased mass spectrometry-based analyses. To obtain true snapshots of intracellular metabolites, leakage-free sample pretreatment and unbiased metabolite determination are required. For cell acquisition, suspension cells could be directly centrifuged to obtain cell pellets while the adherent cells must be detached before metabolite extraction. The adherent growth cells can be harvested by scraping or using trypsin. Traditionally, trypsin was often used to harvest cells. However, previous studies have concluded that harvesting cells by trypsinization lead to the loss of a large amount of metabolites [18, 19]. Therefore,

direct quenching of cells with physical scraping was used as an alternative. However, this was not conducive to cell counting. To address this, measuring the protein content of cell pellets to correct the number of cells has been reported as a promising method for standardizing cell culture systems [20]. Metabolite quenching is the first critical step in the sample preparation process. The quenching process should meet several requirements: the enzyme activity must be quenched as quickly as possible to avoid metabolite degradation and changes in sample composition. Some metabolites are extremely unstable with a short turnaround time, such as adenosine triphosphate (ATP) and glucose 6-phosphate (G6P) [21], so rapid quenching procedure is essential to ensure the true state of intracellular metabolites [22]. Quenching can usually be achieved by freezing samples in liquid nitrogen [23], or in cold methanol solution [24]. It has been reported that cold methanol quenching caused serious metabolite leakage in cell, resulting in an overall loss of metabolite recovery [25]. However, in cancer cells, a systematic evaluation of the extent of metabolite leakage among different quenchers and the influential factors giving rise to it has rarely been reported.

Besides leakage-free quenching method, a complete extraction of intracellular metabolite is required. In previous studies, a lot of efforts have been devoted to the development of extraction methods for intracellular metabolites in different mammalian cells. For instance, Sellick et al. used 100% methanol extraction twice and then water once to extract the metabolites, which could recover the largest range of intracellular metabolites from Chinese hamster ovary (CHO) cells [26]. However, at the same time, other extraction method should be required to maximize the non-polar metabolites recovered. Dettmer et al. used methanol/water to scrap cells harvest and extract metabolites from adherently growing SW480 cells [18]. Wamelink et al. used 50% acetonitrile to extract intermediates in pentose phosphate pathway in fibroblasts and lymphoblasts [27]. However, these extraction methods have not yet been evaluated together with quenching procedures to develop a generalized protocol for acquiring intracellular metabolome in mammalian cells. Furthermore, obtaining accurate concentrations of intracellular metabolites were of great significance for the validation of metabolic fluxes and the establishment of metabolic models [22, 28, 29]. Mass spectrometry such as Gas Chromatography-Mass Spectrometry (GC-MS) and Liquid Chromatography tandem Mass Spectrometry (LC-MS/MS) has been widely used in the determination of metabolites due to its high accuracy and high resolution [30, 31]. However, sample recovery needs to be determined experimentally for each analyte. To circumvent this, the stable isotope internal standard of the analyte was the best choice, because the substance could be distinguished by mass spectrometry, and IDMS could be used to track and correct the loss of the sample during pretreatment and analysis [32]. The stable isotope internal standards could be cultivated on a medium with uniformly labeled ^{13}C -glucose as the sole carbon source, and the ^{13}C -labeled internal standard of intermediate metabolites and target metabolites could be obtained through the self-metabolism of microbial cells [33]. By combining GC-MS/LC-MS/MS with the IDMS method, it is possible to track losses during sample pretreatment and analytical process [32, 33] and greatly increase the accuracy of metabolite quantitation. Furthermore, previously developed sample preparation methods were merely developed for 2D adherent cells, which cannot be directly applied to 3D tumor model without further evaluation. As is known, the 2D cells cannot simulate the complex structure and heterogeneity of tumor tissue in vivo [34, 35]. 3D multicellular tumor spheroids (3D MTSs) are a tumor model between 2D monolayer cell culture and animal models [36]. Compared with traditional 2D model, the internal concentration gradient of nutrients and oxygen led to outer proliferation of living cells, inner accumulation of necrotic cells and living quiescent cells in the transition zone [37]. This inhomogeneity is an important feature of solid tumors in vivo. Many anticancer drugs exert cytotoxic effects on proliferating cells, while quiescent cells escape treatment [38, 39]. Therefore, model systems such as 3D MTS involving quiescent cells are critical for preclinical drug screening and drug resistance investigations.

In this study, we systematically evaluated 12 sample preparation protocols for accurate determination of intracellular metabolites in both 2D and 3D tumor cell models. Further, based on the optimal sample preparation protocol, quantitative metabolomics analysis was used to discover the differential metabolome features of both 2D and 3D tumor models in response to DOX treatment.

2. Materials and methods

2.1 Cell lines and media

HeLa carcinoma cells were purchased from American Type Culture Collection (ATCC, Manassas, VA, USA). Cells were cultured in dulbecco's modified eagle medium (DMEM) (Gibco, 11995-065, USA) supplemented with 10% fetal bovine serum (Gibco, 10099-141, USA), 100 IU/mL penicillin and 100 mg/mL streptomycin (B540732, Sangon Biotech, Shanghai, CN). Cells were maintained in 75 cm² flasks in a 37°C, 5% carbon dioxide incubator (Thermo Fisher Scientific, Waltham, MA, USA) and passaged when the confluence of cells reached 80%–90%.

2.2 Rapid generation of single tumor spheroid

To aggregate cells into a spheroid, cells in the exponential growth phase were digested with 2.5% trypsin, diluted to 10,000 cells/mL, quickly mixed with 2.5% volume fraction of Matrigel (356,237, Corning, NY, USA), and seeded into a "U" type ultra-low attachment 96-well plate (Corning 7007, USA) at 200 μ L/well. The 96-well plates were then centrifuged at 1000 \times g for 10 min, and incubated in a 37°C, 5% CO₂ incubator.

2.3 The addition of DOX

2D monolayer culture: 2D cells were cultured at a seeding density of 3.5×10^5 cells/mL for 48 h. 3D MTS: HeLa cells were cultured at a density of 2000 cells/well for 6 days. Then removed the medium and incubated with 1 μ M DOX (dissolved in medium) for 48 h.

2.4 Preparation of uniformly ¹³C-labeled cell extract

Pichia pastoris G/DSEL strains were cultivated with ¹³C fully-labeled glucose as the sole carbon source, and to increase the intracellular abundance of metabolites in the central carbon metabolism, the ¹³C fully-labeled glucose pulses were applied. The detailed operating procedures was performed as described earlier [40]. The prepared cell extracts were split and stored at -80°C pending for use. The extracts (100 μ L) mentioned above were added before intracellular metabolite extraction. Based on the IDMS theory, this internal standard could track the loss of metabolites during sample pretreatment and MS-based analytical process [41].

2.5 Quenching and extraction procedures for intracellular metabolites

2D Hela cells were harvested after 48 h of incubation. The growth medium was removed and the flasks were washed by 5 mL PBS twice to remove extracellular metabolites. In all experiments, 2D cells were quenched on the flask surface and then scraped with extraction solvent. Cells were quenched and metabolites were extracted using 12 combinations of quenching and extraction methods as described below (**Figure 1**).

MTSs were harvested at 6th day and collected in 10 mL centrifuge tubes. The cell suspension was centrifuged at 1000 \times g for 5 min, the media was removed and the cell pellet was washed twice with 5mL PBS to remove extracellular metabolites. Then the MTSs were digested with Accutase cell digestive solution (40506ES60, Yesen, Shanghai, CN) at 37 for 30 min to form single-cell suspension and washed once with PBS. The single cell suspension was centrifuged for 10 min at 1000 \times g and the supernatant was removed.

1. Liquid nitrogen quenching - 80% methanol extraction

After being washed by PBS, 15 mL liquid nitrogen was added to quench the 2D cells for 1 min. Then the sample was added with 3 mL of 80% methanol, and the cells were scraped gently and fully with a cell scraper. The cell suspension was harvested into a 10 mL centrifuge tube and 100 μ L yeast cell extracts as internal standards were added. Then the cell suspension was vortexed for 30 s and quickly frozen in liquid nitrogen. After thawing on ice at 4°C, samples were centrifuged at 1000 \times g for 10 min and the supernatant was collected. The freeze-thaw process was repeated twice. Finally, the cell pellet was extracted by water. For the water extraction, the cell pellet was resuspended in 1 mL ice-cold milliQ water followed by flash freezing in liquid nitrogen. After thawing on ice at 4°C, samples were centrifuged at 12000 \times g for 10 min and the supernatant was collected. The methanol and water extracts were pooled together, centrifuged at 12000 \times g for 10 min and the supernatant was collected and stored at -80 °C.

The cell pellets of MTSs were prepared as mentioned above and collected in 10 mL centrifuge tubes, which were then frozen in liquid nitrogen for 1 min. The subsequent quenching and extraction methods were performed the same as 2D cells.

2. Liquid nitrogen quenching - 50% acetonitrile extraction

The quenching and extraction were performed as described for the Liquid nitrogen quenching-methanol extraction where 80% methanol was replaced by 50% acetonitrile.

3. Liquid nitrogen quenching - 1:1:1 methanol: chloroform: water extraction

The quenching and extraction were also performed as described for the Liquid nitrogen quenching-methanol extraction where 80% methanol was replaced with 1:1:1 methanol: chloroform: water.

4. Liquid nitrogen quenching - 70% ethanol extraction

The quenching step was performed as described above. Then the sample was added with 3 mL of 70% ethanol (75), and the cells were scraped gently and fully with a cell scraper. The cell suspension was harvested into a 10 mL centrifuge tube and 100 μ L internal standards were added. The cell suspension was quickly put in 75°C water for 3 min, then centrifuged at 1000 \times g for 10 min and the supernatant was removed. The cell pellet was resuspended in a 3 mL of the same ethanol solution and the extraction repeated. Finally, the cell pellet was resuspended in 1 mL ice-cold milliQ water followed by 75°C water bath for 3 min. The ethanol and water extracts were pooled together, centrifuged at 12000 \times g for 10 min and the supernatant was collected and stored at -80°C.

5. 50% Methanol quenching - 80% methanol extraction

The cells were rapidly quenched by 10 mL 50% methanol (-40°C). Then the quenching solution was removed and stored at -80. The metabolites were extracted from the cells using the methods as described in 2.5.1.

6. 50% Methanol quenching - 50% acetonitrile extraction

The quenching and extraction were performed as described for the methanol quenching-methanol extraction method as described in 2.5.5 where 80% methanol was replaced with 50% acetonitrile.

7. 50% Methanol quenching - 1:1:1 methanol: chloroform: water extraction

The quenching and extraction were performed as described for the methanol quenching-methanol extraction where 80% methanol was replaced by 1:1:1 methanol: chloroform: water.

8. 50% Methanol quenching - 70% ethanol extraction

The quenching step was performed as described for the methanol quenching. The extraction step was performed as described in 2.5.4.

9. Normal saline quenching - 80% methanol extraction

The cells were rapidly quenched by 10 mL normal saline (0.5degC). Then the supernatant of quenching solution was collected and stored at -80. The metabolites were extracted from the cells using the methods as described in 2.5.1.

10. Normal saline quenching - 50% acetonitrile extraction

The quenching and extraction were performed as described for the normal saline quenching-methanol extraction where 80% methanol was replaced by 50% acetonitrile.

11. Normal saline quenching - 1:1:1 methanol: chloroform: water extraction

The quenching and extraction were performed as described for the normal saline quenching-methanol extraction where 80% methanol was replaced by 1:1:1 methanol: chloroform: water.

12. Normal saline quenching - 70% ethanol extraction

The quenching step was performed as described for the normal saline quenching. The extraction step was performed as described in 2.5.4.

2.6 Total protein versus cell mass as a normalization strategy

In this study, metabolites were quantified based on the weight of total protein. Single cell suspensions from both 2D monolayer culture and 3D MTS were centrifuged for 10 min at 12,000xg at 4. For measurement of total protein amount, the pellets were resuspended in Radio Immunoprecipitation Assay (RIPA) Lysis Buffer (Thermo Scientific, 89901, USA). The protein concentration was determined using a bicinchoninic acid (BCA) assay (Thermo Fischer Scientific, Waltham, MA, USA) following the instructions of manufacturer. 5 μ L each protein lysate was added to 2 μ L reagent A, followed by the addition of 100 μ L reagent B. After 30 min at 37, absorbance was read at 562 nm by fluorescence microplate reader (Thermo Fisher Scientific, Waltham, MA, USA). Protein concentrations in the sample were determined using standard curves generated by linear regression analysis.

2.7 Metabolite sample pretreatment and MS-based analytical procedures

The above-mentioned sample extracts were evaporated to dryness using Rap-Vap (Labconco, Kansas City, MO). The obtained residue was redissolved in deionized water to obtain a final weight of 600 μ g. Subsequently, the extracts were split and stored at -80 until analysis.

Samples for amino acids quantification were analyzed using GC-MS (7890A GC, Agilent, Santa Clara, CA, USA) instrument coupled to a 5975C MSD single quadrupole mass spectrometer (Agilent, Santa Clara, CA, USA). Briefly, 100 μ L cell extracts were freeze-dried and derivatized by adding 75 μ L acetonitrile and 75 μ L N-methyl-N-(tert-butyltrimethylsilyl) trifluoroacetamide (MTBSTFA) at 70°C for 60 min. Then the derivatized sample was cooled to room temperature and centrifuged at 12000xg for 2 min. The supernatant was collected for further analysis.

Samples for organic acids, sugar phosphates, adenosine nucleotides and coenzymes were analyzed using LC-MS/MS (Dionex Ultimate 3000 UPLC system coupled to TSQ Quantum Ultra mass spectrometer, Thermo Scientific). The absolute quantification of these metabolites was achieved using GC-IDMS and LC-MS/MS-IDMS methods [42]. The details of the analytical procedure have been described elsewhere [22].

2.8 Data statistical analysis

All data in this study were expressed as mean \pm standard deviation (SD). Data analysis was performed by GraphPad Prism 8.0. The heatmap was generated using the pheatmap package (R version 4.0.1). The pathway enrichment was performed using the MetaboAnalyst (<https://www.metaboanalyst.ca/>). Significant analysis was performed by GraphPad Prism 8.0, with $p < 0.05$, $p < 0.01$ and $p < 0.001$ indicated that there were significant (*), highly significant (**), and extremely significant (***) difference between the groups, respectively.

3. Results and discussion

3. 1 Define the optimal quenching and extraction procedure for quantitative metabolomics

Accurate determination of intracellular metabolite levels requires well-established procedures for sampling and sample pretreatment. The ideal procedure should immediately quench cellular metabolism and quantitatively extract all metabolites, while a significant challenge associated with the rapid turnover, varied abundance and physicochemical diversity of intracellular metabolites still requires systematic and quantitative evaluation. Otherwise, the obtained biased metabolite level will lead to misinterpretation of functional information about the biochemical and physiological states of cells [40]. In recent years, different quenching and extraction methods have been proposed and used for quantitative metabolomics of mammalian cells including tumor cells (**Table 1**). Early quenching studies on microorganisms established the use of cold methanol as a standard quenching protocol for its high efficiency of freezing enzyme activities [43-45], and cold methanol has also been reported frequently as the quenching agent in mammalian cell metabolomics [20, 24, 46, 47]. In addition to cold methanol, the use of cold normal saline has also become common and

cold 0.9% (w/v) NaCl has been preferably used for quenching mammalian cell metabolism with minimal metabolite leakage [48]. Meanwhile, liquid nitrogen was also a commonly used quenching method in recent years which could rapidly and efficiently stop cell metabolism [18, 49-52]. After cell harvesting and quenching, metabolite extraction was the next critical step. Several methods existed for metabolite extraction, but the literatures were sometimes contradictory regarding the adequacy and performance of each technique [41]. To the best of our knowledge, the polarity of metabolites ranged from very hydrophilic to hydrophobic compounds, and polar metabolites were supposed to be extracted with ethanol, methanol, acetonitrile, or other mixtures of these solvents, etc [18, 24, 26, 46, 48, 51, 52], while more lipophilic metabolites could be extracted by chloroform/methanol/water mixture, etc [20, 47, 49]. At the same time, in order to ensure that the extraction of intracellular metabolites was as complete as possible, the extraction was usually combined with several freeze-thaw cycles [18].

However, no previous study has yet simultaneously optimized these critical procedures, i.e., quenching and extraction, to explore cell metabolomics using a strictly quantitative approach. Therefore, in this study, we systematically evaluated 12 combinations of three commonly used quenchers and four extractants using an IDMS approach and the specific experimental workflow were shown in **Figure 1**. The prepared samples were analyzed using gas/liquid chromatography-IDMS method, and a total of 43 metabolites were quantitatively determined in Hela cells, including amino acids, sugar phosphates, organic acids, adenosine nucleotides and coenzymes (**Figure 2**).

As shown in **Figure 1**, the medium was first removed and the cells attached to the flask surface were washed twice with PBS. The conventional method generally used trypsin to detach cells from their growth surface, which has been proven to inevitably change the profile of cellular metabolites since the detachment of cells from the extracellular matrix altered their physiology [18, 53-55]. In order to avoid changing the cellular environment before quenching metabolic activities within the cell, in this study, tumor cells cultivated in 2D mode were directly quenched and then scraped with the extraction solvent in all experiments. Meanwhile, 3D MTSs were first digested into single cell suspension, and the cell pellet was obtained after centrifugation. The subsequent operations were the same as those of the 2D cells. We estimated the cell number by determining the protein content of cell pellet. The standard curve of the protein was shown in **Figure S1**. With respect to quenching efficiency, ideal quenching solvent should immediately inhibit cellular metabolic activity and inactivate enzymes within the cells without leaking metabolites from the cells. Quenching of metabolism was usually achieved by rapid changes in temperature or pH. The rate of quenching was critical because many metabolic reactions in glycolysis, as well as those related to ATP, featured high turnover rates in the timescale of seconds [45]. Numerous studies have reported the adverse effects of prolonged exposure to quenching solutions which demonstrated that the longer the cells were exposed to the quenching solution, the exacerbated leakage of intracellular metabolites [22, 45, 56]. This seemed reasonable that prolonged exposure to organic solvents and cold shock could cause cell membrane leakage, which also implied that sample processing should proceed as quickly as possible to the extraction step. In addition, quantitative methods should be used to determine the extent of cellular leakage so that true intracellular metabolite concentrations could be determined [45]. To achieve this, we quantitatively assessed the number and amount of leaked metabolites in the quenching agent, and investigated the factors that influenced the extent of leaked metabolites.

In order to determine the most effective extraction method, four different extraction methods were evaluated after Hela cells were quenched with liquid nitrogen, 50% methanol, and normal saline respectively. The evaluated extraction methods included 80% methanol, 50% acetonitrile, methanol: chloroform: water (1:1:1, v/v/v) and 70% ethanol (75). Sellick et al. found that the addition of a water-based extraction step combined the properties of solvent-based and water-based methods, and extracts produced in this method showed the greatest amount of recovered metabolites in CHO cell [26]. Therefore, we also adopted an additional water extraction to increase metabolite coverage for all 12 combination methods. The metabolites in the obtained cell extracts were absolutely quantified using GC-IDMS and LC-MS/MS-IDMS method. Subsequently, effectiveness of the quenching and extraction procedures should be quantitatively evaluated for their suitability for Hela carcinoma cells grown as 2D monolayer cultures and 3D MTS. For this purpose, previous

studies have reported some evaluation criteria with respect to relative metabolite abundance and metabolite coverage. For example, LORENZ et al. established a method for relative quantification of metabolites in adherent mammalian cells using the clonal β -cell line INS-1 as a model sample, without considering absolute quantification of metabolites [49]. Dietmair et al. evaluated several quenching and extraction procedures for mammalian cells grown in suspension, but did not take into account the reproducibility of each method, with large errors in the metabolite level [48].

To allow an accurate view of intracellular metabolome, the quenching step should stop metabolism as quickly as possible while the extraction should cover a wide spectrum of metabolite. Furthermore, target metabolites should not undergo any physical or chemical modification and degradation should be minimized during quenching and extraction process [45]. In this study, we evaluated the compatibility of three different quenchers such as liquid nitrogen, -40°C 50% methanol, 0.5°C normal saline and four extractants (80% methanol, methanol:chloroform: water (1:1:1, v/v/v), 50% acetonitrile, 75°C 70% ethanol) for global metabolite profiling of adherent Hela carcinoma cells. To comprehensively evaluate 12 combinations of quenching and extraction procedures in this study, we analyzed the acquired metabolite data based on the following four criteria: 1) Metabolite leakage in the quenching solution; 2) Metabolite coverage and abundance identified in cell extracts; 3) Absolute quantitation of intracellular metabolite concentrations; 4) Reproducibility of metabolite quantification [57].

3.1.1 Metabolite leakage in the quenching solution

To study the effect of quenching solutions on the integrity of cell membrane, the potential metabolite leakage during quenching was evaluated by quantifying the metabolites in the quenching solution. The metabolites analyzed include compounds with different properties, such as amino acids, organic acids, sugar phosphates, adenosine nucleotides and coenzymes. **Figure 3** showed the effect of these two quenchers (50% methanol and normal saline) on the recovery of different representative metabolites. Liquid nitrogen did not cause intracellular metabolites leak into the quencher because liquid nitrogen would volatilize directly. In both cases, all determined amino acids were found in the quenching solution. Compared with normal saline, cold methanol gives rise to more serious leakage of intracellular amino acids (**Figure 3a**). Also, an obvious phenomenon showed that the more leakage comes with the higher amounts of intracellular amino acids, such as alanine (Ala), valine (Val), proline (Pro), lysine (Lys), aspartate (Asp), glutamate (Glu). In consistency with amino acids, organic acids, sugar phosphates and energy metabolism intermediates also exhibited a significant higher leakage when tumor cells were quenched with the cold methanol. Meanwhile, the results also indicated that intracellular sugar phosphates were more inclined to leak in response to cold methanol treatment (**Figure 3b**). According to previous reports, the higher degree of leakage caused by cold methanol may be partly attributed to the following aspects. The first was the increase in cell membrane fluidity or the decrease in thickness during the quenching process [57]; The sudden increase in cell membrane permeability caused by "cold shock" was also reported [58]; In addition, methanol was a small molecule which was easier to penetrate cells which may also be the reason for the leakage of intracellular metabolites [22]. Moreover, Canelas et al. found that the extent of metabolite leakage in *S. cerevisiae* was affected by the methanol content of the quencher, and reducing the methanol concentration resulted in the increase of intracellular metabolite leakage [44]. Therefore, the necessity of fine-tuning quenching strategy should be emphasized. In general, it could be concluded that methanol quenching was not suitable for accurate quantification of the metabolites in Hela cells. Normal saline was the better of the two quenchers, although it could not completely prevent leakage.

Furthermore, we investigated the factors such as the molecular weight which has been reported to affect the degree of metabolite leakage [56]. **Figure 4** showed the relationship between the degree of metabolite leakage and molecular size which was represented by molecular weight. We found that metabolites with a smaller molecular weight were more seriously leaked than metabolites with a larger molecular weight when normal saline was used as the quencher. This was consistent with the findings by Canelas et al. observed in *S. cerevisiae* that the leakage of the metabolites into the quenching solution was mostly driven by diffusion [56] and the diffusion rate of smaller molecules was higher [44]. In contrast with this, when cold methanol was

used as the quencher, the degree of metabolite leakage showed no clear relation with the molecular weight, and severe leakage was observed to be widespread in the detected metabolites.

3.1.2 Metabolite coverage and abundance identified in cell extracts

The comparison of quantitative whole-cell metabolites showed that the number and total amount of metabolites extracted under each condition were significantly different (**Figures 5 and 6**). For example, Oxaloacetic acid (OAA) was below the detection limit with methanol/chloroform as the extractant, but detectable in all the other extractants. Most sample preparation procedures frequently used cold organic solvents to stop cellular metabolic activities. In this study, we also quenched cellular metabolism directly by adding liquid N₂ on the flask plate, followed by the addition of extraction solvent. Our results showed relatively less metabolites were obtained with methanol as the quencher compared to cells quenched with normal saline or directly quenched with liquid N₂. Kapoor et al. also found that methanol quenching treatments resulted in severe leakage of nearly all metabolite classes in metastatic breast cancer cell line MDA-MB-231 [29]. In addition to this, the result also showed that direct quenching with liquid N₂ produced the highest recovery of all metabolites compared with methanol and normal saline (**Figure 6**). Additionally, the overall effect of normal saline as the quenching agent was between liquid nitrogen and methanol. Consistently, one previous study also reported that quenching with 60% methanol (buffered or unbuffered) resulted in leakage of intracellular metabolites from the cells. Whereas, quenching with cold normal saline (0.9% [w/v] NaCl, 0.5) did not damage the cells and effectively prevented the conversion of ATP to adenosine diphosphate (ADP) and adenosine monophosphate (AMP), indicating metabolic arrest in CHO cells [48].

Furthermore, based on the number of metabolites extracted, acetonitrile shows the best extraction efficiency (**Figure 5**). In addition to the total number of extracted metabolites, the total amount of extracted metabolites was also an important indicator for evaluating the extraction methods. The results showed that using liquid nitrogen as the quencher and 50% acetonitrile as the extractant, the maximum total amount of intracellular metabolites could be harvested, about 295 nmol/million cells, which was 1.67 times to 13.73 times higher than other combination methods. In addition, it could be observed that this optimal method allowed a high extraction capacity for adenosine nucleotides and coenzymes (**Figure 6**). For the four different extractants, it can be inferred that the extraction efficiency of acetonitrile and ethanol was generally higher, while the extraction efficiency of methanol: chloroform: water (1:1:1, v/v/v) (M/C) was the worst regardless of the type of quenchers (**Figure 6**).

3.1.3 Absolute quantitation of intracellular metabolite concentrations

The absolute concentration of the intracellular metabolites was used to compare the efficiency of extraction solvents. We found that different extraction solvents differed in extraction efficiencies of specific intracellular metabolites. In terms of amino acid recovery, we analyzed 18 amino acids by GC-MS and observed a clear trend for amino acids. The largest amount of amino acids was extracted when the liquid nitrogen as the quenching agent and 50% cold acetonitrile as the extractant. However, the extraction of amino acids with cold methanol as the quenching agent was very poor, which was caused by the serious leakage of amino acids mentioned above. Also, methanol/chloroform (M/C) had a poor extraction effect on intracellular amino acids. This may be ascribed to the weak polarity of methanol/chloroform and low solubility of amino acids. M/C extraction, which was originally used to extract non-polar metabolites [59], such as fatty acids [18]. Hot ethanol extraction was proved to be as effective as acetonitrile for amino acid recovery, but there were differences in the selective recovery of specific amino acids such as serine (Ser), aspartate (Asp), asparagine (Asn) (**Figure 7**). Overall, amino acids were more soluble in water-based extractions (methanol, acetonitrile, and hot ethanol) which was consistent with previous study [26].

For organic acids and sugar phosphates, cold methanol as the quencher also behaved poor extraction effects and extracted the least amount. The recovery of fumarate (FUM), oxaloacetate (OAA) and phosphoenolpyruvic acid (PEP) was relatively low regardless of the type of extractants. For the rest organic acids such as pyruvic acid (PYR), malate (MAL) and α -ketoglutarate (α KG), using cold methanol and hot ethanol as the extractant can achieve better extraction results. Among sugar phosphates, the extraction effects of

glyceraldehyde 3-phosphate (G3P), 3-phosphoglycerate (3PG), erythrose-4-phosphate (E4P) and fructose-1,6-bisphosphate (FBP) were generally poor. When liquid nitrogen and acetonitrile was used as the quencher and the extractant respectively, the extraction amount of 6-phosphogluconate (6PG) and sedoheptulose-7-phosphate (S7P) was the highest, and the extracted S7P even reached about 5.89 nmol/million cells, which was 8.96 times to 295.69 times higher than other extraction methods. This method was also suitable for the extraction of glucose-6-phosphate (G6P) and fructose-6-phosphate (F6P) which was only slightly less than normal saline quenching - 80% methanol extraction (S-M) and liquid nitrogen quenching - 80% methanol extraction (N₂-M) (**Figure 8**).

Finally, high temperature in some extraction methods might affect the recovery of thermally unstable metabolites. Nevertheless, in our study, we did not observe that hot ethanol obviously caused the adverse effect regarding the number and amount of detected metabolites (**Figure 8**). One previous study has reported that several metabolites (PYR, nucleotides and sugar phosphates) were unstable in hot ethanol [22]. However, Sellick et al. found that hot ethanol had a good performance on recovering fatty acids such as stearic acid and palmitic acid because of the increased solubility of fatty acids [26]. To demonstrate the specific effects of heat extraction, we focused on the levels of the labile metabolite nicotinamide adenine dinucleotide (NAD) (**Figure 8**). The recovery of intracellular NAD clearly showed that liquid nitrogen quenching - 50% acetonitrile extraction (N₂-A) and normal saline quenching - 50% acetonitrile extraction (S-A) recovered relatively larger amounts of NAD, hot ethanol extraction was slightly inferior, but better than methanol and M/C as extractants. In our study, M/C was poor in the extraction of each metabolite although previous study showed certain advantages in the extraction of cholesterol and fatty acids [57]. Therefore, these data emphasized the importance of using the appropriate quenching-extraction process for the extraction of specific metabolites. An ideal extraction method should recover the metabolites as much as possible; however, one extraction method in general was not capable of allowing a complete metabolite extraction. For this purpose, a combined extraction process might be an alternative to increase the number and amount of metabolites. However, the reduction of accuracy and reproducibility of the combination method in extraction was also an undisputable fact, which largely offsets its advantage in enhancing the metabolite spectrum [57].

3.1.4 Reproducibility of metabolite quantification

To evaluate the reproducibility of the methods detected, we used average relative standard deviation (RSD) as an indicator to evaluate the reproducibility of the extraction solvent. The RSD results of 43 metabolites obtained using 12 combinations of quenching and extraction methods were shown in **Table 2**. The introduction of ¹³C internal standards allowed us to quantitatively evaluate extraction methods with regard to biological reproducibility. In 2D HeLa cells, the difference between the average RSD values of different methods was not significant, mostly between 20%-30%. S-A method had the lowest average RSD (18.9%) while the N₂-M/C method had the largest average RSD (39.9%). The average RSD of the N₂-A method which behaved excellent regarding metabolite coverage and abundance was 27.8%. The RSD values of 11 methods (except N₂-M/C) were below 30%, indicating good reproducibility independent of quenching and extraction procedures. In addition, in all methods (except N₂-M/C), the percentage of individual metabolites with RSD <30% was higher than 58% (**Table 3**). Guenther et al. found that in HCT116 cells, the percentages of metabolites with RSD < 30% cultured in 10% and 20% fetal calf serum (FCS) conditions using different quenching solvents, extraction ratios were ranging from 0% to 79% which had a large error [20]. In our study, the percentage of individual metabolites with RSD <30% for the optimal N₂-A method could reach 61.0%, and the largest percentage of individual metabolites with RSD <30% of all methods was 69.9%, which proved that our methods were reproducible for most metabolites and N₂-A method was relatively stable for the extraction of metabolites detected. By analyzing the RSDs of 12 methods, we found that the sample preparation methods using liquid N₂ as the quenching agent had higher RSDs than the other two quenching agents, and the proportion of metabolites with RSDs less than 30% was also lower. We speculated that this might be caused by the difficulty in accurately determining the added volume and the volatilization time of liquid nitrogen, which made it impossible to ensure complete consistency of the quenching time (the contact time between samples and quenching agents) between parallel samples. However, for the metabolites with

RSDs \leq 50%, there were only three metabolites in N₂-A method, which was the fewest among all 12 methods.

3.2 Validation of the optimal quenching - extraction procedure on 3D MTSs

3D tumor spheroids are important model systems due to the capability of capturing in vivo tumor complexity. To our knowledge, few relevant studies have ever reported comprehensive evaluation of intracellular metabolite extraction of 3D MTSs. To date, only a few metabolomics studies have been dealt with 3D MTS models [60, 61]. Despite showing strong potential for combining 3D MTSs and metabolomics study, a detailed protocol for obtaining absolute metabolome was far from complete. For example, Rusz et al. used the HCT116 3D MTS model for the experimental design of a metabolomics workflow. The established protocol consisted of a quick wash of the spheroids on the plate followed by extraction with cold methanol [51]. However, it was uncertain whether this method was suitable for the extraction of intracellular metabolites from 3D MTS in a leakage-free manner. In addition, this protocol has not been quantitatively validated and also has not been applied to 2D adherent cells for broad applicability. In this study, sample preparation protocols developed with 2D monolayer cultures were extended to acquire single spheroid metabolomics. We aimed to investigate whether the best sample preparation protocol for 2D cells was also applicable to 3D MTSs. The preparation method of tumor spheroids followed the steps as described in **Material and methods 2.2**. As the incubation time increased, the spheroid became rounder and bigger (**Figure S2A**). On the 6th day, the MTS reached a plateau with a maximum diameter of $538.26 \pm 7.19 \mu\text{m}$, the roundness of the MTSs exceeded 0.9, and the number of viable cells of a single MTS reached the maximum, about 34000 ± 1000 (**Figure S2B**). The morphology and microstructure of the 6th day MTSs were observed with a scanning electron microscope (SEM), and it was found that the MTSs had a good 3D structure (**Figure S2C**). After 6 days of culture, tumor spheroids were collected and the intracellular metabolites were obtained using the above-mentioned 12 combinations of quenching and extraction methods.

The experimental results demonstrated that in 3D MTSs, the leakage of intracellular metabolite with methanol as the quencher was more serious than that of normal saline, which was the same as that found in 2D cells (**Figure 9**). Also, the same conclusion was drawn with 3D tumor spheroid metabolomics analysis that the degree of metabolite leakage was associated with molecular weight (**Figure S3**). For the 12 quenching-extraction methods, N₂-A method was also the best method applied to 3D MTSs in terms of the number and amount of intracellular metabolites extracted (**Figure S4**). Moreover, the percentage of intracellular metabolites with RSD less than 30% in 3D MTSs for the N₂-A method can reach 48.7% (**Table S2**). However, we found the average RSD values of each metabolite from 3D MTSs were significantly higher ($P < 0.01$) than that from 2D cells as a whole (**Figure S5**), which might be ascribed to the fact that some small cell clusters in single cell suspension (**Figure S6**) have a certain impact on the reproducibility of metabolite extraction. This might be solved by extending the enzymatic hydrolysis time to reduce cell clusters, but long-time exposure to Accutase cell digestive solution likely affects membrane integrity and permeability and causes the leakage of intracellular metabolites, which needed to be verified by subsequent experiments. Taken above, our study showed that the optimized sample preparation protocol (N₂-A method) developed for the intracellular metabolite extraction of 2D adherent cancer cells can be well applied to 3D MTSs.

3.3 Assessing the intracellular metabolic changes of Hela cells exposed to DOX

The above results arrive at the conclusion that N₂-A has been identified as the most optimal method to acquire intracellular metabolites with minimal loss during Hela carcinoma sample preparation. Metabolomics is emerging as an important tool for understanding the molecular mechanisms underlying the response of drug delivery systems. Further, in this study, a case study with the acquired intracellular metabolomics data from Hela carcinoma cell under both 2D monolayer culture and 3D MTS in response to anticancer drug DOX treatment was illustrated using this optimal sample preparation protocol. DOX is a kind of anti-tumor antibiotics widely used in clinics and prevents the resealing of DNA double helix and subsequently creates a double stranded DNA break which leads to cell death [62-64]. In our study, we focused on the intracellular metabolite changes of Hela cells exposed to DOX. We determined the cytotoxicity of the drug to 2D monolayer culture and 3D MTSs through cell counting kit-8 (CCK-8). As shown in **Figure S7**, compared with the 2D control, 3D MTSs showed higher resistance to DOX treatment. After 48 hours of

DOX treatment, the half maximal inhibitory concentration (IC_{50}) values of 3D MTSs and 2D monolayer culture cells were 13.13 μ M and 1.108 μ M, respectively. As expected, the result indicated that 3D Hela MTSs were less sensitive to DOX than 2D monolayer cells.

As shown in **Figure 10**, extracellular concentrations of glucose, lactic acid, glutamine and ammonia were measured. It has been acknowledged that cancer cells rely on aerobic glycolysis instead of mitochondrial respiration for the rapid provision of ATP and precursors, a phenomenon termed “the Warburg effect” [65]. Apparently, 3D cells consumed more glucose for aerobic glycolysis and produced a larger amount of lactate as compared to 2D cells (**Figure 10**). Therefore, 3D MTSs conserved a more tumor metabolic phenotype in terms of Warburg effect. After adding 1 μ M DOX in 2D cells, extracellular glucose was hardly consumed, and the level of lactate remained basically unchanged, which was around 0.2 g/L with the dosing time. By contrast, the ability of 3D MTSs to consume glucose and produce lactic acid was significantly stronger than 2D cells. This might indicate that the addition of DOX had a greater impact on the respiration capacity of 2D cells than 3D cells. In addition, it was found that when glucose and glutamine were present at the same time, cancer cells preferably used glutamine first. The addition of DOX did not change the utilization of glutamine in both 2D and 3D cells. Regarding ammonia metabolism, the ammonia produced by 2D cells was gradually accumulated, while 3D cells accumulated ammonia in the early stage of culture, and re-consumed ammonia in the later stage of culture. This seemed reasonable because metabolic recycle of ammonia has been reported to favor tumor cell growth [6].

After the DOX treatment, the hierarchical cluster analysis of the acquired intracellular metabolites showed that the treatment on 3D MTSs elicited more pronounced metabolic changes than 2D monolayer cultures (**Figure 11**). Specifically, 2D monolayer cells before and after dosing showed significant regulation on 13 metabolites among which G3P, proline (Pro) and pyruvate (PYR) were upregulated while glycine (Gly), ribose-5-phosphate (R5P), serine (Ser), nicotinamide adenine dinucleotide phosphate (NADP), glutamine (Gln), NAD, cysteine (Cys), aspartate (Asp), threonine (Thr), and malate (MAL) were down-regulated. In contrast, 24 metabolites were significantly changed in 3D MTS after dosing with DOX, where citrate (CIT), G3P, Ser, Cys, Ala, Thr, glutamine, valine, and lysine were up-regulated while PYR, Glu, 3PG, succinate (SUC), NAD, 6PG, NADP, leucine (Leu), AMP, ATP, AKG, Pro, Asn, E4P, and PEP were down-regulated. Armiñán et al. found that 2D MCF7 cells exposed to free DOX reduced the intracellular levels of Gly, NAD and Asp, which was consistent with our findings in 2D Hela cells [66]. Previous studies have also shown that reduced levels of Gly (2D) and Glu (3D) were associated with reduced glycolysis [67], and Gly in particular has been considered as a biomarker for cancer prognosis and treatment response [68]. To corroborate this, extracellular metabolite data revealed that glucose uptake and lactate production were inhibited in both 2D and 3D cells after exposure to DOX, which also indicated a reduced glycolysis (**Figure 10**). Interestingly, the intracellular Gln pool showed different trends in 2D and 3D cells after dosing with DOX. Glutamine was an important source of carbon in cells. Glutaminolysis was necessary for cancer cells to satisfy the need to replenish TCA cycle intermediates and to produce NADPH [69]. For 2D cells, the addition of DOX reduced the glycolytic flux and the intracellular glutamine concentration, indicating that the cells may be insufficient to replenish the TCA cycle through glutamine, resulting in the death of 2D cells; while for 3D cells, intracellular glutamine concentration was observed increased, indicating that glutamine was sufficient to maintain the replenishment requirements of the TCA cycle when the cells were reduced in glycolysis.

As shown in **Figure 12**, pathway enrichment analysis using targeted metabolomics data showed that differential pathways for 2D and 3D cells after doses of DOX were associated with redox stress, such as glutathione metabolism (2D: Glycine/NADP⁺/L-Cysteine/Acetyl-CoA/L-Glutamate down-regulated, 3D: NADP⁺/L-Glutamate down-regulated, L-Cysteine up-regulated), purine metabolism (2D: D-Ribose 5-phosphate/L-Glutamine down-regulated, 3D: ADP/AMP/ATP down-regulated, L-Glutamine up-regulated), nicotinate and nicotinamide metabolism (2D: NADP⁺/L-Aspartate down-regulated, 3D: NADP⁺/NAD⁺ down-regulated). Oxidative stress signifies the imbalance between the production of reactive oxygen species (ROS) and antioxidant defenses, which could lead to apoptosis and is accompanied by a lot of metabolic alterations. Metabolic changes associated with redox stress, including downregulation of Gly (2D) and ATP (3D), have been implicated in oxidative stress-induced aging [70]. In addition, previous study has also showed that there

appeared to be a link between the reduction of NAD levels and the induction of oxidative stress [71]. To verify this, we also measured ROS of HeLa cells (2D cells and 3D MTSS) before and after dosing with DOX (**Figure S8**). Our results were consistent with the putative DOX targeting mechanism of action and the increase in redox stress where ROS has been confirmed by previous studies as the main cause of cytotoxicity [62]. In addition to this, the results also showed that DOX exposure would significantly affect amino acid metabolism-related pathways (Glycine, serine and threonine metabolism, cysteine and methionine metabolism, arginine and proline metabolism, and alanine, aspartate and glutamate metabolism) in both 2D and 3D cells. Triba et al. observed the simultaneous decrease of glutamine and alanine after DOX-treated in B16-F10 cells which was interpreted as a drug-induced transient switch from glycolysis to oxidative phosphorylation to supply ATP, and further initiate apoptosis [72]. Previous studies have also reported that apoptosis might be associated with increased levels of branched-chain amino acids (valine, leucine, and isoleucine) and decreased levels of alanine [66]. Finally, the metabolomics data of this study also indicated the common pathway enrichment, which had been reported on other drugs, such as purine and pyrimidine metabolism. For example, Rusz et al. found that exposure to oxaliplatin affected purine metabolism and pyrimidine synthesis, which was in accordance with the ribosome biogenesis stress recently proposed as the primary cause for the cytotoxic effects [51].

4. Conclusion

In this study, we systematically evaluated 12 combinations of quenching and extraction methods for acquiring quantitative intracellular metabolome with both 2D and 3D HeLa carcinoma models based on the isotope dilution mass spectrometry method. Our results showed that liquid nitrogen as quenching agent and 50% acetonitrile as extracting agent was proven to be the most optimal method to acquire intracellular metabolome for both 2D HeLa and 3D MTSS. Based on this, a quantitative metabolomics study showed that DOX exposure gave rise to pronounced metabolite changes between 2D and 3D HeLa carcinoma models. Strikingly, our data suggested that compared to 2D cells the increased intracellular glutamine level in 3D cells can benefit replenishing the TCA cycle when the glycolysis was limited after dosing with DOX.

In summary, this study provides a well-established quenching and extraction protocol for quantitative metabolome profiling of HeLa carcinoma cell under 2D and 3D cell culture conditions. Based on this, quantitative time-resolved metabolite data can serve to the generation of hypotheses on metabolic reprogramming to reveal its important role in tumor development and treatment.

Acknowledgement

This work was financially sponsored by State Key Laboratory of Bioreactor Engineering, Scientific Research Think Tank of Biological Manufacturing Industry in Qingdao (QDSWZK202004), the Fundamental Research Funds for the Central Universities (Grant No. JKJ01211515) and the 111 project (Grant No. B18022).

Conflict of Interest

The authors declare no conflict of interest.

Data availability statement: Data available on request from the authors

5. References

- [1] Sung, H., Ferlay, J., Siegel, R. L., Laversanne, M., *et al.*, Global cancer statistics 2020: GLOBOCAN estimates of incidence and mortality worldwide for 36 cancers in 185 countries. *CA: a cancer journal for clinicians* 2021, *71*, 209-249.
- [2] Tomasetti, C., Li, L., Vogelstein, B., Stem cell divisions, somatic mutations, cancer etiology, and cancer prevention. *Science* 2017, *355*, 1330-1334.
- [3] Pavlova, N. N., Thompson, C. B., The emerging hallmarks of cancer metabolism. *Cell Metab* 2016, *23*, 27-47.

- [4] Cairns, R. A., Harris, I. S., Mak, T. W., Regulation of cancer cell metabolism. *Nat Rev Cancer* 2011, *11* , 85-95.
- [5] Patra, K. C., Wang, Q., Bhaskar, P. T., Miller, L., *et al.* , Hexokinase 2 is required for tumor initiation and maintenance and its systemic deletion is therapeutic in mouse models of cancer. *Cancer Cell* 2013, *24* , 213-228.
- [6] Spinelli, J. B., Yoon, H., Ringel, A. E., Jeanfavre, S., *et al.* , Metabolic recycling of ammonia via glutamate dehydrogenase supports breast cancer biomass. *Science* 2017, *358* , 941-946.
- [7] Gong, Y., Liu, Z., Yuan, Y., Yang, Z., *et al.* , PUMILIO proteins promote colorectal cancer growth via suppressing p21. *Nat Commun* 2022, *13* , 1-17.
- [8] Wang, T.-H., Wu, C.-C., Huang, K.-Y., Leu, Y.-L., *et al.* , Integrated Omics Analysis of Non-Small-Cell Lung Cancer Cells Harboring the EGFR C797S Mutation Reveals the Potential of AXL as a Novel Therapeutic Target in TKI-Resistant Lung Cancer. *Cancers* 2020,*13* , 111.
- [9] Lubes, G., Goodarzi, M., GC-MS based metabolomics used for the identification of cancer volatile organic compounds as biomarkers. *J Pharmaceut Biomed Analysis* 2018, *147* , 313-322.
- [10] Mayers, J. R., Wu, C., Clish, C. B., Kraft, P., *et al.* , Elevation of circulating branched-chain amino acids is an early event in human pancreatic adenocarcinoma development. *Nat Med* 2014,*20* , 1193-1198.
- [11] Mayers, J. R., Torrence, M. E., Danai, L. V., Papagiannakopoulos, T., *et al.* , Tissue of origin dictates branched-chain amino acid metabolism in mutant Kras-driven cancers. *Science* 2016, *353* , 1161-1165.
- [12] do Valle, Í. F., Menichetti, G., Simonetti, G., Bruno, S., *et al.* , Network integration of multi-tumour omics data suggests novel targeting strategies. *Nat Commun* 2018, *9* , 1-10.
- [13] Jain, M., Nilsson, R., Sharma, S., Madhusudhan, N., *et al.* , Metabolite profiling identifies a key role for glycine in rapid cancer cell proliferation. *Science* 2012, *336* , 1040-1044.
- [14] Newman, A. C., Maddocks, O. D., Serine and functional metabolites in cancer. *Trends Cell Biol* 2017, *27* , 645-657.
- [15] Tao, L., Zhou, J., Yuan, C., Zhang, L., *et al.* , Metabolomics identifies serum and exosomes metabolite markers of pancreatic cancer. *Metabolomics* 2019, *15* , 1-11.
- [16] Garcia-Bermudez, J., Baudrier, L., La, K., Zhu, X. G., *et al.* , Aspartate is a limiting metabolite for cancer cell proliferation under hypoxia and in tumours. *Nat Cell Biol* 2018, *20* , 775-781.
- [17] León, Z., García-Canaveras, J. C., Donato, M. T., Lahoz, A., Mammalian cell metabolomics: experimental design and sample preparation. *Electrophoresis* 2013, *34* , 2762-2775.
- [18] Dettmer, K., Nurnberger, N., Kaspar, H., Gruber, M. A., *et al.* , Metabolite extraction from adherently growing mammalian cells for metabolomics studies: optimization of harvesting and extraction protocols. *Anal Bioanal Chem* 2011, *399* , 1127-1139.
- [19] Bi, H., Krausz, K. W., Manna, S. K., Li, F., *et al.* , Optimization of harvesting, extraction, and analytical protocols for UPLC-ESI-MS-based metabolomic analysis of adherent mammalian cancer cells. *Anal Bioanal Chem* 2013, *405* , 5279-5289.
- [20] Fritsche-Guenther, R., Bauer, A., Gloaguen, Y., Lorenz, M., Kirwan, J. A., Modified Protocol of Harvesting, Extraction, and Normalization Approaches for Gas Chromatography Mass Spectrometry-Based Metabolomics Analysis of Adherent Cells Grown Under High Fetal Calf Serum Conditions. *Metabolites* 2019, *10* , 2.
- [21] Weibel, K. E., Mor, J.-R., Fiechter, A., Rapid sampling of yeast cells and automated assays of adenylate, citrate, pyruvate and glucose-6-phosphate pools. *Anal Biochem* 1974, *58* , 208-216.

- [22] Liu, X., Wang, T., Sun, X., Wang, Z., *et al.* , Optimized sampling protocol for mass spectrometry-based metabolomics in *Streptomyces*. *Bioresourc Bioprocess* 2019, *6* , 1-12.
- [23] Garcia-Canaveras, J. C., Lopez, S., Castell, J. V., Donato, M. T., Lahoz, A., Extending metabolome coverage for untargeted metabolite profiling of adherent cultured hepatic cells. *Anal Bioanal Chem* 2016, *408* , 1217-1230.
- [24] Sellick, C. A., Hansen, R., Maqsood, A. R., Dunn, W. B., *et al.* , Effective quenching processes for physiologically valid metabolite profiling of suspension cultured mammalian cells. *Anal Chem* 2009, *81* , 174-183.
- [25] Jang, C., Chen, L., Rabinowitz, J. D., Metabolomics and isotope tracing. *Cell* 2018, *173* , 822-837.
- [26] Sellick, C. A., Knight, D., Croxford, A. S., Maqsood, A. R., *et al.* , Evaluation of extraction processes for intracellular metabolite profiling of mammalian cells: matching extraction approaches to cell type and metabolite targets. *Metabolomics* 2010, *6* , 427-438.
- [27] Wamelink, M. M., Struys, E. A., Huck, J. H., Roos, B., *et al.* , Quantification of sugar phosphate intermediates of the pentose phosphate pathway by LC-MS/MS: application to two new inherited defects of metabolism. *J Chromat B* 2005, *823* , 18-25.
- [28] Liu, X., Sun, X., Wang, T., Zhang, X., *et al.* , Enhancing candidicin biosynthesis by medium optimization and pH stepwise control strategy with process metabolomics analysis of *Streptomyces ZYJ-6*. *Bioprocess Biosyst Eng* 2018, *41* , 1743-1755.
- [29] Kapoore, R. V., Coyle, R., Staton, C. A., Brown, N. J., Vaidyanathan, S., Influence of washing and quenching in profiling the metabolome of adherent mammalian cells: a case study with the metastatic breast cancer cell line MDA-MB-231. *Analyst* 2017, *142* , 2038-2049.
- [30] Varga, E., Glauner, T., Berthiller, F., Krska, R., *et al.* , Development and validation of a (semi-) quantitative UHPLC-MS/MS method for the determination of 191 mycotoxins and other fungal metabolites in almonds, hazelnuts, peanuts and pistachios. *Anal Bioanal Chem* 2013, *405* , 5087-5104.
- [31] Buescher, J. M., Moco, S., Sauer, U., Zamboni, N., Ultrahigh performance liquid chromatography- tandem mass spectrometry method for fast and robust quantification of anionic and aromatic metabolites. *Anal Chem* 2010, *82* , 4403-4412.
- [32] Mashego, M., Wu, L., Van Dam, J., Ras, C., *et al.* , MIRACLE: mass isotopomer ratio analysis of U-13C-labeled extracts. A new method for accurate quantification of changes in concentrations of intracellular metabolites. *Biotechnol Bioeng* 2004, *85* , 620-628.
- [33] Wu, L., Mashego, M. R., van Dam, J. C., Proell, A. M., *et al.* , Quantitative analysis of the microbial metabolome by isotope dilution mass spectrometry using uniformly 13C-labeled cell extracts as internal standards. *Analy Biochem* 2005, *336* , 164-171.
- [34] Badea, M. A., Balas, M., Hermenean, A., Ciceu, A., *et al.* , Influence of Matrigel on Single- and Multiple-Spheroid Cultures in Breast Cancer Research. *SLAS Discov* 2019, *24* , 563-578.
- [35] Lin, R. Z., Chang, H. Y., Recent advances in three-dimensional multicellular spheroid culture for biomedical research. *Biotechnol J* 2008, *3* , 1172-1184.
- [36] Hirschhaeuser, F., Menne, H., Dittfeld, C., West, J., *et al.* , Multicellular tumor spheroids: an underestimated tool is catching up again. *J Biotechnol* 2010, *148* , 3-15.
- [37] Mehta, G., Hsiao, A. Y., Ingram, M., Luker, G. D., Takayama, S., Opportunities and challenges for use of tumor spheroids as models to test drug delivery and efficacy. *J Control Release* 2012, *164* , 192-204.
- [38] Stewart, D. J., Mechanisms of resistance to cisplatin and carboplatin. *Crit Rev Oncol Hemat* 2007, *63* , 12-31.

- [39] Costa, E. C., de Melo-Diogo, D., Moreira, A. F., Carvalho, M. P., Correia, I. J., Spheroids Formation on Non-Adhesive Surfaces by Liquid Overlay Technique: Considerations and Practical Approaches. *Biotechnol J* 2018, *13* , 1700417.
- [40] Wang, G., Chu, J., Zhuang, Y., van Gulik, W., Noorman, H., A dynamic model-based preparation of uniformly-¹³C-labeled internal standards facilitates quantitative metabolomics analysis of *Penicillium chrysogenum*. *J Biotechnol* 2019, *299* , 21-31.
- [41] Canelas, A. B., ten Pierick, A., Ras, C., Seifar, R. M., *et al.* , Quantitative evaluation of intracellular metabolite extraction techniques for yeast metabolomics. *Anal Chem* 2009, *81* , 7379-7389.
- [42] Wordofa, G. G., Kristensen, M., Schrubbers, L., McCloskey, D., *et al.* , Quantifying the metabolome of *Pseudomonas taiwanensis* VLB120: evaluation of hot and cold combined quenching/extraction approaches. *Anal Chem* 2017, *89* , 8738-8747.
- [43] de Koning, W., van Dam, K., A method for the determination of changes of glycolytic metabolites in yeast on a subsecond time scale using extraction at neutral pH. *Anal Biochem* 1992, *204* , 118-123.
- [44] Canelas, A. B., Ras, C., Ten Pierick, A., van Dam, J. C., *et al.* , Leakage-free rapid quenching technique for yeast metabolomics. *Metabolomics* 2008, *4* , 226-239.
- [45] Winder, C. L., Dunn, W. B., Schuler, S., Broadhurst, D., *et al.* , Global metabolic profiling of *Escherichia coli* cultures: an evaluation of methods for quenching and extraction of intracellular metabolites. *Anal Chem* 2008, *80* , 2939-2948.
- [46] Munger, J., Bajad, S. U., Collier, H. A., Shenk, T., Rabinowitz, J. D., Dynamics of the cellular metabolome during human cytomegalovirus infection. *PLoS Pathog* 2006, *2* , e132.
- [47] Teng, Q., Huang, W., Collette, T. W., Ekman, D. R., Tan, C., A direct cell quenching method for cell-culture based metabolomics. *Metabolomics* 2009, *5* , 199-208.
- [48] Dietmair, S., Timmins, N. E., Gray, P. P., Nielsen, L. K., Kromer, J. O., Towards quantitative metabolomics of mammalian cells: development of a metabolite extraction protocol. *Anal Biochem* 2010, *404* , 155-164.
- [49] Lorenz, M. A., Burant, C. F., Kennedy, R. T., Reducing time and increasing sensitivity in sample preparation for adherent mammalian cell metabolomics. *Anal Chem* 2011, *83* , 3406-3414.
- [50] Lane, A. N., Fan, T. W.-M., Quantification and identification of isotopomer distributions of metabolites in crude cell extracts using 1 H TOCSY. *Metabolomics* 2007, *3* , 79-86.
- [51] Rusz, M., Rampler, E., Keppler, B. K., Jakupec, M. A., Koellensperger, G., Single Spheroid Metabolomics: Optimizing Sample Preparation of Three-Dimensional Multicellular Tumor Spheroids. *Metabolites* 2019, *9* , 304.
- [52] Dubuis, S., Baenke, F., Scherbichler, N., Alexander, L. T., *et al.* , Metabotypes of breast cancer cell lines revealed by non-targeted metabolomics. *Metab Eng* 2017, *43* , 173-186.
- [53] Zhang, K., Zhang, X., Bai, Y., Yang, L., *et al.* , Optimization of the sample preparation method for adherent cell metabolomics based on ultra-performance liquid chromatography coupled to mass spectrometry. *Anal Methods* 2019, *11* , 3678-3686.
- [54] Kapoore, R. V., Coyle, R., Staton, C. A., Brown, N. J., Vaidyanathan, S., Cell line dependence of metabolite leakage in metabolome analyses of adherent normal and cancer cell lines. *Metabolomics* 2015, *11* , 1743-1755.
- [55] Rushing, B. R., Schroder, M., Sumner, S. C., Comparison of Lysis and Detachment Sample Preparation Methods for Cultured Triple-Negative Breast Cancer Cells Using UHPLC–HRMS-Based Metabolomics. *Metabolites* 2022, *12* , 168.

- [56] de Jonge, L. P., Douma, R. D., Heijnen, J. J., van Gulik, W. M., Optimization of cold methanol quenching for quantitative metabolomics of *Penicillium chrysogenum*. *Metabolomics* 2012,8 , 727-735.
- [57] Shin, M. H., Lee, D. Y., Liu, K.-H., Fiehn, O., Kim, K. H., Evaluation of sampling and extraction methodologies for the global metabolic profiling of *Saccharophagus degradans*. *Anal Chem* 2010,82 , 6660-6666.
- [58] Carnicer, M., Canelas, A. B., Ten Pierick, A., Zeng, Z., *et al.* , Development of quantitative metabolomics for *Pichia pastoris*. *Metabolomics* 2012, 8 , 284-298.
- [59] Floch, J., A simple method for the isolation and purification of total lipids from animal tissues. *J. biol. Chem.* 1957,226 , 497-509.
- [60] Fan, T. W., El-Amouri, S. S., Macedo, J. K. A., Wang, Q. J., *et al.* , Stable Isotope-Resolved Metabolomics Shows Metabolic Resistance to Anti-Cancer Selenite in 3D Spheroids versus 2D Cell Cultures. *Metabolites* 2018, 8 , 40.
- [61] Vorrink, S. U., Ullah, S., Schmidt, S., Nandania, J., *et al.* , Endogenous and xenobiotic metabolic stability of primary human hepatocytes in long-term 3D spheroid cultures revealed by a combination of targeted and untargeted metabolomics. *FASEB J* 2017, 31 , 2696-2708.
- [62] Roychoudhury, S., Kumar, A., Bhatkar, D., Sharma, N. K., Molecular avenues in targeted doxorubicin cancer therapy. *Future Oncol* 2020, 16 , 687-700.
- [63] Mizutani, H., Tada-Oikawa, S., Hiraku, Y., Kojima, M., Kawanishi, S., Mechanism of apoptosis induced by doxorubicin through the generation of hydrogen peroxide. *Life Sci* 2005, 76 , 1439-1453.
- [64] Lorenzo, E., Ruiz-Ruiz, C., Quesada, A. J., Hernandez, G., *et al.* , Doxorubicin induces apoptosis and CD95 gene expression in human primary endothelial cells through a p53-dependent mechanism. *J Biol Chem* 2002, 277 , 10883-10892.
- [65] Jang, M., Kim, S. S., Lee, J., Cancer cell metabolism: implications for therapeutic targets. *Exp Mol Med* 2013,45 , e45.
- [66] Arminan, A., Palomino-Schatzlein, M., Deladriere, C., Arroyo-Crespo, J. J., *et al.* , Metabolomics facilitates the discrimination of the specific anti-cancer effects of free-and polymer-conjugated doxorubicin in breast cancer models. *Biomaterials* 2018, 162 , 144-153.
- [67] Yang, Y., Li, C., Nie, X., Feng, X., *et al.* , Metabonomic studies of human hepatocellular carcinoma using high-resolution magic-angle spinning 1H NMR spectroscopy in conjunction with multivariate data analysis. *J Proteome Res* 2007, 6 , 2605-2614.
- [68] Mirbahai, L., Wilson, M., Shaw, C. S., McConville, C., *et al.* , 1H magnetic resonance spectroscopy metabolites as biomarkers for cell cycle arrest and cell death in rat glioma cells. *Int J Biochem & Cell Biol* 2011, 43 , 990-1001.
- [69] DeBerardinis, R. J., Sayed, N., Ditsworth, D., Thompson, C. B., Brick by brick: metabolism and tumor cell growth. *Current Opini Genet Develop* 2008, 18 , 54-61.
- [70] Zeng, J., Liu, J., Yang, G.-Y., Kelly, M. J., *et al.* , Exogenous ethyl pyruvate versus pyruvate during metabolic recovery after oxidative stress in neonatal rat cerebrocortical slices. *Journa American Society of Anesthesiologists* 2007, 107 , 630-640.
- [71] Klawitter, J., Klawitter, J., Gurshtein, J., Corby, K., *et al.* , Bezielle (BZL101)-induced oxidative stress damage followed by redistribution of metabolic fluxes in breast cancer cells: A combined proteomic and metabolomic study. *Int J Cancer* 2011, 129 , 2945-2957.
- [72] Triba, M., Starzec, A., Bouchemal, N., Guenin, E., *et al.* , Metabolomic profiling with NMR discriminates between biphosphonate and doxorubicin effects on B16 melanoma cells. *NMR Biomed* 2010,23 ,

1009-1016.

Table 1 . Reported sample preparation procedures for metabolomics analysis of cultured mammalian cells.

Cell type	Rinse
Human rhabdomyosarcoma cells	Trypsinization/three times with ice-cold PBS
Fibroblasts	No
CHO	No
MCF-7 and MDA-MB-231 cells	Twice with ice-cold phosphate-buffered saline (PBS, pH 7.4)
HCT116	Once with PBS
HCT116	Washed (20 s) with washing buffer (140 mM NaCl, 5 mM HEPES, pH 7.4,
Breast cancer cell lines	Washed twice with a washing solution (75 mM ammonium carbonate, adju
CHO	No
SW480	No
“λοναλ β-σελλ λινε ΙΝΣ-1	37 °C deionized water (2 s)
Recombinant CHO cell line Super-CHO	Washed twice with PBS at room temperature

Table 2 The average RSD of the intracellular metabolites of 2D Hela cells using 12 combinations of quenching and extraction methods.

Methods	N ₂ -M	N ₂ -A	N ₂ -M/C	N ₂ -E	M-M	M-A	M-M/C	M-E	S-M	S-A	S-M/C
Average RSD (%)	27.5	27.8	39.9	20.2	24.5	26.4	26.2	24.4	25.5	18.9	26.0

Table 3 The percentage of intracellular metabolites with RSD less than 30% in 2D Hela cells using 12 combinations of quenching and extraction methods.

Methods	N ₂ -M	N ₂ -A	N ₂ -M/C	N ₂ -E	M-M	M-A	M-M/C	M-E	S-M	S-A	S-M/C	S-E
RSD (%) ≥ 30	58.5	61.0	39.0	78.0	75.6	73.2	68.3	75.6	73.2	82.9	73.2	73.2

Figure legends

Figure 1 Schematic diagram of the sampling, quenching and extraction procedures for Hela cells from 2D monolayer cultures and 3D MTS.

Figure 2 Parameters evaluated during the optimization of metabolome extraction and analysis conditions. The cell collection procedure remains constant for all different combinations of metabolome quenching, extraction and GC/LC-MS analysis. Metabolic quenching is achieved by adding quenchers to the cells. Then, cell separation and metabolite extraction are performed at the same time by scraping the cells in different extraction solvents.

Figure 3 Comparison of the leakage degree of metabolites in different quenchers. (a) The leakage degree of amino acids in different quenchers; (b) The leakage degree of organic acids, phosphate sugars, adenosine nucleotide and coenzymes in different quenchers. Values were the mean of three biological replicates. Error bars represented standard deviation.

Figure 4 The relationship between the degree of leakage and molecular weight in 2D cells. The degree of leakage was calculated based on the level of metabolites in the quencher and the overall metabolite level (quencher + extractant).

Figure 5 The total number of metabolites obtained by each extraction method.

Figure 6 The sum of the different kind metabolites identified in cell extracts only in 2D cells. Significant analysis was performed against N₂-A group.

Figure 7 Eighteen amino acids were identified in 12 quenching-extraction methods. Values were the mean of three biological replicates. Error bars represented standard deviation.

Figure 8 Eight organic acids, nine sugar phosphates, eight adenosine nucleotides and coenzymes were identified in twelve extraction methods. Values were the mean of three biological replicates. Error bars represented standard deviation.

Figure 9 The application of 12 intracellular extraction methods on 3D MTSs. (A) Heat map of the degree of leakage of the two quenchers in 3D MTSs; (B) 43 metabolites were identified in twelve extraction methods in 3D MTSs.

Figure 10 The measured concentrations of extracellular: glucose, glutamine, ammonium and lactate. The culture time of 2D cells and 3D MTSs was shown on the bottom and top axis, respectively.

Figure 11 Heat map of the absolute amount of metabolites. The 2D/3D cells were treated with a medium containing 1 μ M of DOX for 48 h.

Figure 12 Kyoto Encyclopedia of Genes and Genomes (KEGG) pathways affected by DOX using pathway enrichment with the MetaboAnalyst pathway analysis module.



figures/Figure-2/Figure-2-eps-converted-to.pdf

figures/Figure-3/Figure-3-eps-converted-to.pdf

figures/Figure-4/Figure-4-eps-converted-to.pdf

figures/Figure-5/Figure-5-eps-converted-to.pdf

figures/Figure-6/Figure-6-eps-converted-to.pdf

figures/Figure-7/Figure-7-eps-converted-to.pdf

figures/Figure-8/Figure-8-eps-converted-to.pdf

figures/Figure-9/Figure-9-eps-converted-to.pdf

figures/Figure-10/Figure-10-eps-converted-to.pdf

figures/Figure-11/Figure-11-eps-converted-to.pdf

figures/Figure-12/Figure-12-eps-converted-to.pdf